Springer

KSME

Journal of Mechanical Science and Technology 32 (6) (2018) 2569~2575
www.springerlink.com/content/1738-494x(Print)/1976-3824(Online)
DOI 10.1007/s12206-018-0514-0

Modeling of friction-stir butt-welds and its application in automotive bumper impact performance Part 1. Thermo-mechanical weld process modeling †

Sachin Patil[1,*], Yi Yang Tay[1], Farzad Baratzadeh[1,2] and Hamid Lankarani[1]

[1]*Wichita State University, Wichita, KS, USA*
[2]*Advanced Joining and Processing Laboratory, National Institute for Aviation Research, Wichita, KS, USA*

(Manuscript Received May 18, 2017; Revised December 12, 2017; Accepted February 26, 2018)

Abstract

The demand for better structural performance in joining of components for road vehicles prompts the implementation of aluminum alloy friction stir welding technology in the automotive industry. The aim of current study is the creation of a 3-D finite element (FE) friction thermal model and stir welding (FSW) process of dissimilar aluminum alloy and for the estimation of crash worthiness performance of FSW fabricated shock absorber assembly. Thermo mechanical simulations and analysis are performed to understand the thermal behavior in the FSW weld zones. The developed models are correlated against published experimental results in terms of temperature profile of the weld zone. The developed models are then implemented for fabricating vehicle bumper parts to illustrate the performance of FSW welded components during an impact. Customary sled testing for low-speed guard necessities is performed utilizing a grating blend welded test apparatus at Wichita State University (WSU) at the National Institute for Aviation Research (NIAR). A few guard congregations are then appended to the test installation utilizing FSW and conventional Gas bend GMAW welding strategies. Numerical models are likewise created where limited component investigation is utilized to contrast the anticipated harm and the real harm maintained by both of the FSW and GMAW manufactured guards. During the research, a new FSW weld mold is created that allows for a better representation of the desired progressive crack propagation. The FSW fabricated bumper based on the Johnson-Cook failure model yields better failure prediction and is in good agreement to the test. The results from this study provide a guideline for an accurate finite element modeling of a FSW fabricated components and their application in the crashworthiness of such structural components.

Keywords: Friction stir butt welding; Thermal modeling; Johnson-cook failure model; Sled test; Vehicle bumper assembly

1. Introduction

The primary incentive for the increased use of aluminium alloy in auto body structures is the drastic improvement in the structural performance while reducing the weight of the vehicle with less distortion. FSW technology is by far the most promising joining process used in automotive manufacturing. The capability to predict deformation and failure is crucial to automotive body design. A potential problem in the application of this spinoff technology is cracking near welds when automotive body is subjected to large nonlinear strain rate dependent deformation during an impact event. Because separation of welds can affect the crash response of welded structural components, the dynamic behaviour of the FSW fabricated components has been one of the critically important considerations in vehicle design and manufacturing [1].

There are a number of factors which can affect the mechanical responses of a FSW welded structure due to thermal mechanical interaction. This makes it essential to study heat generation during welding process. In terms of simulating the heat generation during FSW process, Schmidt et al. [2] proposed a model for predicting heat profile based on the nature of the contact at the tool matrix interface namely sliding, sticking or partial sticking conditions. Contrary, several studies were focused on heat conduction and ignored the plastic flow around the tool [3, 4]. In terms of classical formulations based on analytical models, Chen et al. [5] and Zhang et al. [6] introduced a three-dimensional model simulated using finite element analysis to study the thermal history and thermo-mechanical process in the butt-welding process. Friggard et al. [7] assumed frictional heating at the tool shoulder/work piece interface for the heat generation during welding. They estimated heat generated from the friction at the tool shoulder interface using inverse modeling. The relationship between friction and thermal properties has also been characterized by

*Corresponding author. Tel.: +1 316 2001716
E-mail address: sapatil1@shockers.wichita.edu
† Recommended by Associate Editor Choon Yeol Lee

various researchers [8, 9]. Song and Kovacevic [10] developed a transient three-dimensional thermal model of AA6063 alloy. They estimated the partitioning of heat at the tool/work piece interface by an iterative numerical method. Ulysse [11] modeled the large plastic deformation involved in stir-welding processes by relating the deviatoric stress tensor to the strain-rate tensor. The thermo-mechanical affected zone (TMAZ) was assumed to be a rigid-visco-plastic material where the flow stress depends on the strain rate and temperature. The heat generation rate term were shown to be expressed as the product of the effective stress and effective strain-rate.In this work, temperature-dependent conductivity and specific heat coefficients for aluminum alloys were adopted. The temperature distributions in the tool were compared with experimental results. Based on this study, thermo-mechanical FE model developed for identifying heat evolved using LS-DYNA. This is moving heat source analysis. Heat input from friction stir welding can be described using a distributed heat source based on the Gaussian distribution of power in space proposed by Goldak et al. [12]. Khandkar et al. [13] presented an input torque based thermal model for FSW of AA6063-T6 alloy. Their objective was to predict the thermal history and temperature distribution during FSW for a butt joint. In their study, the moving heat source represented by the heat generated by tool rotation and linear traverse of the shoulder and pin has been correlated to the torque data obtained from experiment.

Most of previous researchers who have been studied FSW has focused more on investigating thermal modelling. It is also necessary to study strength of weld joint and consequences of weld strength after manufacturing welded parts. In order to answer this research question FSW weld joints are analysed macroscopically for vehicle structure.Prior to this, first phase of study focuses on understanding the heat generation in the welding process and presents briefly the 3D simulations of FSW welding. Further FSW development work includes microstructural examination to evaluate weld strength and analyzing the performance of weld modeling.

As mentioned in literature survey that FSW is subjected to large nonlinear strain rate dependent deformation during an impact event. This nonlinear strain rate dependent response is due mainly to the weld constituent. Therefore, constitutive relationship are developed for FSW weld in terms of hardness and thermal history and experimentally verified in this study. A typical FSW thermal model was studied using dynamic field tests and finite element analysis. Additionally, there is limited information for FSW joints between dissimilar metal joining of AA6082-T6 and AA6063-T6. The AA6063-T6 is highly weldable and derives its superior mechanical properties from the microstructures as per the thermal cycle of welding than the conventional alloys that are susceptible to forming brittle microstructures and solidification-induced defects in the weld region. Heat affected zone (HAZ) softening can occur in conventional alloys. Therefore, the AA6063-T6 generally has higher load-bearing capacity. The AA6082-T6 is a high strength Al-Mg-Si alloy with good toughness and ductility. Artificial aging in both alloys at 190 °C creates tempering condition to join 4 mm thick plates together to form a bumper and crash-box assembly for impact application. Baratzadeh et al. [14] published their sled test results for FSW joint evaluation for various low speed impact tests. The objective of that study was to assess the structural performance a bumper and crash-box assembly fabricated using FSW and GMAW methods. Testing were performed and FE models were developed to achieve this goal. The bumper and crash-box assembly are impacted on a rigid wall at four impact velocities 7, 10, 15 and 20 kph. As a subsequent evaluation of this approach, failure analysis of FSW butt weld has been applied in dealing with impacts of vehicle structure against rigid barriers.

Overall for the goal of the current study on characterizing the mechanical behavior of FSW weld, this study is divided into two phases, namely:

(1) Integrated thermo-mechanical weld process modeling to generate the weld geometry microstructure.

(2) Comparison of weld characterization and impact test database for development and validation of the weld modeling approach.

A possible extension of this would be to cover a wider range of Al alloy materials joining, and microstructures to validate and demonstrate this methodology for implementation by the auto industry users.

2. FSW butt weld modeling and simulation

The goal of initial phase is to create the thermal model of Friction stir weld valid for the butt joints of AA6063-T6 and AA6082-T6 alloy plates and correlate with available experimental cases published in Ref. [14]. This initial modeling approach is focused on approximate estimation of heat generated during the FSW process. The thermal modeling and simulation of FSW is developed in nonlinear finite element code Ls-Dyna. Thermal material property identification defined in the *MAT_THERMAL card. The thermal properties must be specified for all solid, shell and thick shell parts if a thermal or coupled thermal structural/analysis is being performed. The purpose of the thermal model is to calculate the transient temperature fields developed during welding process.

In the thermal analysis, the transient temperature field T, which is a function of time t and the spatial coordinates (x, y, z), is estimated by the three-dimensional nonlinear heat transfer equation. The thermal model responsible for the temperature field T is governed by

$$k\left(\frac{\partial^2 T}{\partial x^2}+\frac{\partial^2 T}{\partial y^2}+\frac{\partial^2 T}{\partial z^2}\right)+Q_{\text{int}}=(c\rho\frac{\partial T}{\partial t}) \tag{1}$$

where k is the coefficient of thermal conductivity, Q_{int} is the internal heat source rate, c is the mass-specific heat capacity, and ρ is the density of the materials [15].

Table 1. Material properties of crash-box and bumper.

Components	Materials	Density (kg/m^3)	Young's modulus (GPa)	Proof stress (GPa)	Tensile strength (GPa)
Crashbox	AA6063-T6	2700	68.9	0.275	0.317
Bumper	AA6082-T6	2700	70.0	0.280	0.331

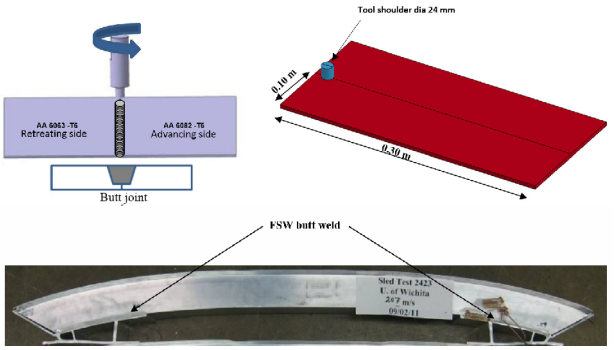

Fig. 1. Geometric model of plate to be welded.

2.1 Model geometry and material properties

Three-dimensional model is developed to carry out parametric study of friction stir welded joint on variation of process parameter such as tool rotational speed and tool travel rate. The heat input from the pin is included. All frictional dissipated energy is converted into heat during load step. The FSW tool is modeled using lagrangian formulation having shoulder diameter (d) and length (l) are 24 mm and 30 mm, respectively. The workpiece material is modeled using the eulerian formulation and is made to move while the tool is rotating at a constant velocity. The domain modeled in the current analysis considered to be of 305 mm × 100 mm × 4 mm. Approximately 120000 elements were used to discretize the eulerian subdomain. Fully coupled thermo- mechanical analysis is carried out. The material flows through the mesh and interacts with the lagrangian tool. The tool rotation speed kept constant 390 rpm for all experiments whereas welding speed is 90, 140, 200 mm/min.

The geometry of plates to be welded is appeared in Fig. 1.

The materials used are AA6063-T6 and AA6082-T6 alloys for butt joint between the bumper and crash box. Mechanical properties of both alloys are shown in Table 1.

The material data is used as input for Ls-Dyna temperature dependent plasticity constitutive Johnson Cook material model [16, 17]. The MAT_JOHNSON_COOK define the equation as:

$$\sigma = \left[A + B\varepsilon^{n}\right]\left[1 + C\ln\dot{\varepsilon}\right]\left[T^{*}\right]^{m} \tag{2}$$

here, A is the plastic strain constant; B the strain hardening constant; C the strain rate constant; n the strain rate exponent; m the thermal exponent; $\dot{\varepsilon}$ is the equivalent plastic strain rate

Table 2. Flow-stress JC model constants in Ls-Dyna [18].

*MAT_JOHNSON_COOK (AA6082-T6)							
MID	RO	G	E	PR	DTF	VP	
1	2.70E-09	2.87E+04	7.47E+04	0.3	0	1	
A	B	N	C	M	TM	TR	EPSSO
352	440	0.42	0.0083	0	775	300	1
CP	PC	SPALL	IT	D1	D2	D3	D4
9.0E+07	1.0E+07	2	1	0	0.65	1.5	0

(effective strain rate divided by $\dot{\varepsilon}_0$ s^{-1}, so that it is also dimensionless), and this is set at 1.0 s^{-1}. T^* is the homologous temperature, which is another dimensionless quantity defined by

$$T^{*} = \frac{T - T_0}{T_M - T_0} \tag{3}$$

where T_0 = 298 K is room temperature and T_M = 934 K is the temperature at which the material melts. In the given sample, the stress flow is based on heat and heat change is evaluated by estimating the adiabatic conditions. By plastic work created heat in an element and the resultant rise in heat is evaluated by making use of specific heat of a given material (905 J/kgK). The influence is understood by defining the little bit of rate of dissipation which is inelastic and which generally comes as per volume flux of heat. The Johnson-Cook visco-plastic model has five material parameters each representing an independent material property of the work material. Calibration of the modified JC material model constant done using Voce hardening rule and Excel macro prepared to determine Johnson-Cook parameters. These parameters have a bearing on the flow stress outcome which has an effect on the accuracy of the modeling process. JC strength model constants for AA6082-T6 are shown in Table 2. The equation constants for the AA6063-T6 are A=261.2 MPa, B = 126.8 MPa, n = 0.0862, m = 1.34 and C = 0.301; and for AA6082-T6 are A = 352 MPa, B = 140 MPa, n = 0.2, m = 1.21 and C = 0.0023.

To better define the material properties, an equation of state used. The linear polynomial equation of state is linear in internal energy (E). The pressure (P) is given by:

$$P = C_0 + C_1\mu + C_2\mu^2 + C_3\mu^3 + (C_4 + C_5\mu + C_6\mu^2)E\,. \tag{4}$$

*EOS_LINEAR_POLYNOMIAL is utilized by setting C1 to the bulk modulus and all the other C terms to zero [18]. In this equation, μ is constant referring to density ratio. The heat source is steel rigid and the material model *MAT _020_RIGID is used. The tool has angular velocity of 390 rpm and plunge velocity of 140 mm/sec [19]. Thermal material property identification (TMID in *PART card) characterized in *MAT_THERMAL card to enable the thermal conditions.

2.2 Loading and boundary conditions

Due to the inflow and the outflow nature used in the boundary conditions, volume fraction defined in the eulerian domain initially for each element. This was accomplished through the use of the appropriate inflow and outflow velocity boundary conditions over the vertical faces of the Eulerian domain which are orthogonal to the direction of tool travel. Thermal boundary conditions are symmetrical across the weld centerline. Tool shoulder/workpiece boundary condition is a Neumann heat flux boundary condition and is calculated from frictional heat [5]. The heat generated by friction between the workpiece and tool shoulder is the only source of heat generation. The total heat input Q in watts for this model is calculated from equations provided by Frigaard et al. [7] and is applied as a moving heat flux through Ls-Dyna code that uses Goldak's moving heat source model [12]. The heat period Q and its rate at the interface amongst the top of work piece and shoulder is an element of frictional coefficient μ, rotational speed N, and span of shoulder R.

$$Q = \frac{4}{3}\mu\pi^2 NR^3. \tag{5}$$

The *BOUNDARY_THERMAL_WELD card being used to characterize the properties of various weld region.*INITIAL_TEMPERATURE_SET is utilized to determine the underlying procedure temperature of the model. The heat source is characterized by the *BOUNDARY_FLUX card. The dimensions for the tool is obtained from Khandkar et al. [13] for correlation to the published research data. The tool angular rotation is 390 rpm and the applied downward force on tool is set at 22.4 kN and tool travel rate was 140 mm/min. A frictional coefficient of 0.4 is found to give comparable results in the present study for all simulation conditions. These values were in conformity with a large number of published research data. Heat fluxes or convections (but not both) can be input as surface loads at the element. A convective coefficient of 32 W/(m^{2}K) at the bottom surface of the sheet is assumed for a butt weld to account for the conduction between the sheets and the backup plate. Additionally, a convection coefficient of 5 W/(m^{2}K) was applied at all the surfaces except the bottom surface. These assumptions were consistent with other researcher's model methodology [3, 8, 13] and yielded good comparison between simulated and experimental data. However additional testing to define the thermal pathways and thermal conductance would allow use of models for more general applications.

2.3 Contact definitions

Contact condition help to model process forces during welding cycle and to compute the thermal history of the contact interfaces. In this model, the concept of thermal contact conductance (TCC) is used based on the works of Zahedul et al. [19] and Xu and Khan [20] and. As discussed in the introduction, they developed this concept (TCC) because the contact resistance between the faying surfaces dictates the overall thermal history and this value is directly proportional to the pressure applied on the tool.

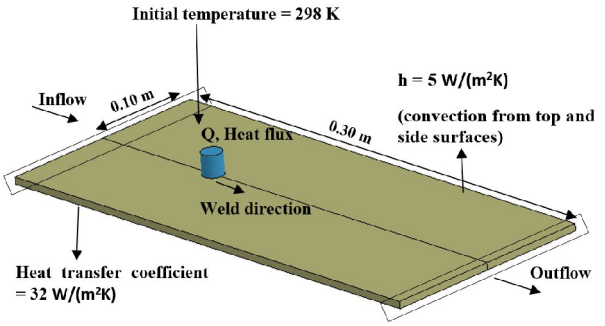

Fig. 2. Representation of boundary conditions [13].

$$\text{TCC} = \text{HTCo} \times \rho \tag{6}$$

where HTCo is the basic Heat Transfer Contact conductance, where 2 × 10^6 W/m°C is calculated for this study using an equation developed by Madhusudana [21] and ρ is the dimensionless pressure distribution factor. The thermal contact conductance used between the sheets varies from 2 × 10^6 W/m°C for the region immediately outside tool shoulder area by a factor of 10.

3. Results and discussion

The developed thermo-mechanical model was verified with numerical results obtained by Zahedul et al. [19]. The FE temperature predictions are slightly higher than the actual joining temperatures when compared to experimental results due to dissimilar alloy joining in this study. Measurements of temperatures are recorded through the application of embedded thermocouples at 25 different positions on the bottom to top surfaces at the work piece along the transverse section. The figure shows a graph of comparing test and simulation outcomes for the work piece's top surface. The measurement for work piece temperature was done and estimated along the transverse dimension at weld line.

In Fig. 3, the maximum top surface experimental temperature of 430 °C was matched equally to the modeled temperature and is about 75 % of the melting temperature (580 °C) of Al6062-T6 aluminum alloys. The peak temperature at the edge of sheet was 90 °C which matched the modeled temperature at that point. The overall trend was similar in both experimental and numerical case which is required for a good correlation. Some difference in between experimental and numerical temperature was seen due to material parameters used in simulation, assumption of boundary conditions and frictional coefficients, etc. Asymmetrical temperature distribution around weld centerline is observed due to the non-

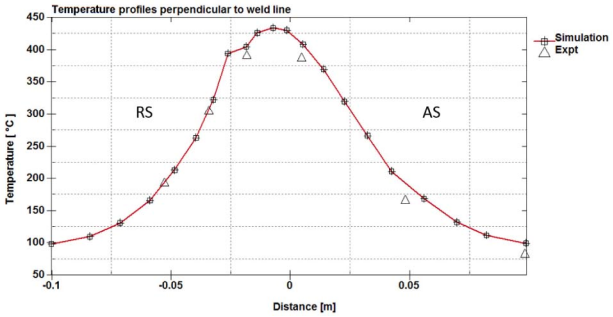

Fig. 3. Simulated and experimental outcomes [19] along traverse direction of AA6063-T6 and AA6082-T6 used at t = 88 s.

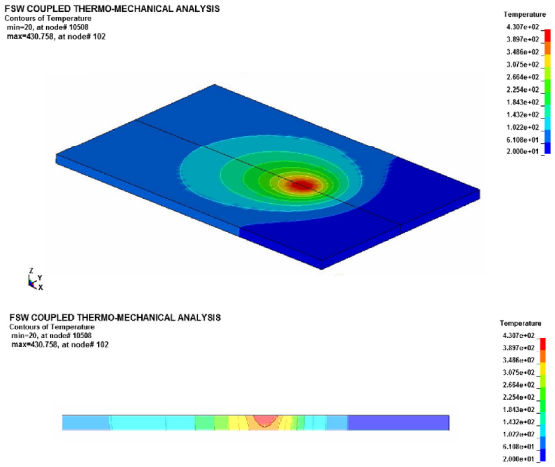

Fig. 4. Temperature contours simulated in Ls-Dyna.

uniform material flow and severe plastic deformation at the advancing side (AS). The energy density is lower to retreading side than advancing side which result in slightly lower temperature for few points on retreading side (RS). This observation is consistent with other studies [12, 19]. A similar trend for bottom and middle surface temperature profiles were observed [22].

3.1 Result summary for FSW of butt weld

In the later part of this work, various other approaches for modeling of FSW studied. After reviewing Refs. [13, 19], choice of a further validation test is performed using Abaqus [23] for butt weld of AA6063-T6 and AW6082-T6. In this analytical model, DFLUX subroutine for moving heat flux setup in Abaqus to model FSW based on the Gaussian moving heat source [24]. To create the Gaussian distribution, volumetric heat flux generated similar to Ls-Dyna heat flux method. Boundary heat flux applied as load in the model with amplitude calculation as a Gaussian moving heat source. This heat source propagated gradually as moving weld tip with the help of Step-2 Heat Transfer defined. Interaction was defined for heat transfer, surface film, surface conduction, radiation, etc. Verification of the thermal modeling results is shown in Fig. 5 capturing the heat flow direction similar to Ls-Dyna model.

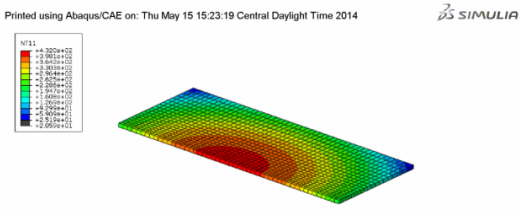

Fig. 5. Thermal steady state results (nodal temperature contours) using Abacus for same input conditions.

Abacus model shows 432 °C nodal temperature at various nodes in weld zone for tool travel rate of 200 mm/min. The variation in temperature is reasonable as seen in figure due to large size of work piece in the Ls-Dyna. As observed, the thermal history provides a better understanding of the process. Unless there is extreme processing parameters are chosen, the maximum temperature usually lies between 425 and 500 °C.

Overall, a key feature of these integrated thermal-mechanical weld process modeling is that it predicts the microstructure evolution based on the calculations of the thermal cycle results of Al alloy phase transformation processes. A work piece has localized high temperature gradient at the center of the nugget. Due to this localized high temperature gradient, the residual stress after the welding process is concentrated around the weld nugget. The mechanical properties such as the Poisson's ratio and Young's modulus vary due to the variation of the temperature in the analysis and is crucial to consider in the application of FSW welded components. This study led to phase 2 which is an in-depth exploration of the material properties in FSW fabricated components [25]. There is no need to experimentally measure the annealing softening in the HAZ, an impossible task for all possible thermal cycles experienced in different locations of the weld and HAZ of a weld. This is because various dislocation structures disappears in recovery and/or recrystallization processes. Thus calculations of the hardness, the volumetric changes associated with the phase transformation are determined using the thermal expansion/contraction of each microstructural constituent. The distributions of microstructures and associated material properties during the entire welding cycle are calculated for each element integration point in both FE model. These detailed microstructure gradient data can be used in the stress calculations to simulate the microstructure evolution during welding. The model dynamic friction coefficient of 0.4 for the butt weld permitted correlation of Ls-Dyna temperature history plots to experimental data. These values were in conformity with a large number of published research data.

The Ls-Dyna FE model is found to be in good agreement with the published results. Moreover, simulation results from Abacus thermal model compared well with the Ls-Dyna results. Table 3 shows the tabulated peak temperature results for butt weld of AA6063-T6 and AA6082-T6. FS butt welding of two Al alloy shows comparatively lower temperature when compared to Zahedul et al. [19] for different tool travel speeds as seen in Table 3. Good weld quality could be obtained for

Table 3. Summary of peak temperatures for butt weld of AA6063-T6 and AA6082-T6.

Material	Tool rotational velocity (rpm)	Tool travel rate (mm/min)	Top surface peak temperature (°C)
AA6063-T6 +AA6082-T6	390	140	470
		200	430
		90	421

peak temperatures in between 420 °C to 510 °C which is possible with welding speeds in the range of 90 mm/min to 200 mm/min for a tool rpm of 390 rpm.

In general, the temperature usually stays below 500 °C. These values must be treated with some care, as the position of the thermocouple in the rapidly moving nugget can be difficult to ascertain during experimental measurements. Microstructural evidence seems to corroborate the thermocouple based experimental result. Moreover, lower heat input are favorable for minimizing the HAZ liquation cracking because they decrease the size of various zones around weld nugget and allow fine grains size to form during weld solidification. This allows weld solidification uniformly and balanced grain size for better weld ability and performance. Coverage of the present review is confined to the FSW of aluminum alloys. Limiting the available heat generation by reducing the torque leading to significant reductions in distortion. Moreover the work piece flow stress and heating of the nugget at the tool/work piece interface will fall rapidly as the tool travel rate lowered.

4. Conclusion

In order to examine the thermal history during the welding process, an initial attempt to develop a fully coupled thermos-mechanical model for FSW was done. With this approach, JC parameters better represented thermal history of weld joint. Material property development in different FSW zones based on thermal results studied in next phase to predict the behavior of the friction stir welded bumper crash box assembly in crash events. The influence of thermal properties in FSW weld region investigated using micro-hardness testing and material model development. FSW produces considerably less heat input than MIG welding [26] for bumper crash box assembly and has been successfully produced on many of the important commercial Al alloys including the 5xxx, 6xxx and 7xxx series.

References

[1] T. Barnes and I. Pashby, Joining techniques for aluminium spaceframes used in automobiles: Part I—solid and liquid phase welding, *Journal of Materials Processing Technology*, 99 (1-3) (2000) 62-71.

[2] H. N. B. Schmidt, J. H. Hattel and J. Wert, An analytical model for the heat generation in friction stir welding, *Modeling and Simulation in Materials Science and Engineering*, 12 (1) (2004) 143-157.

[3] J. E. Gould and Z. Feng, Heat flow model for friction stir welding of aluminum alloys, *Journal of Materials Processing & Manufacturing Science*, 7 (2) (1998) 185-194.

[4] Y. J. Chao and X. Qi, Thermal and thermo-mechanical modeling of friction stir welding of aluminum alloy 6061-T6, *Journal of Materials Processing & Manufacturing Science*, 7 (2) (1998) 215-233.

[5] C. M. Chen and R. Kovacevic, *Finite element modeling of friction stir welding—thermal and thermomechanical analysis*, Research Center for Advanced Manufacturing, Department of Mechanical Engineering, Southern Methodist University, International Parkway, Suite 100, Richardson, TX 75081, USA (2003).

[6] H. Zhang and Z. Zhang, Numerical modeling of friction stir welding process by using rate-dependent constitutive model, *J. Mater. Sci. Technol*., 23 (1) (2007) 73-80.

[7] O. Frigaard, O. Grong, B. Bjorneklett and O. T. Midling, Modeling of the thermal and themicrostructure fields during friction stir welding of aluminum alloys, *1st International Symposium on Friction Stir Welding*, Thousand Oaks, CA, USA, June 14-16 (1999).

[8] O. Lorrain, J. Serri, V. Favier, H. Zahrouni and M. E. Hadrouz, A contribution to a critical review of friction stir welding numerical simulation, *Journal of Mechanics of Materials and Structures*, 4 (2) Feb (2009).

[9] M. J. Russell and H. R. Shercliff, Analytical modelling of friction stir welding, *INALCO '98: 7th International Conference: Joints in Aluminum*, Cambridge, UK, 16 April, 2 (1998) 185-217.

[10] M. Song and R. Kovacecic, Thermal modeling of friction stirs welding in a moving coordinate system and its validation, *Proc. Inst. Mech. Eng. B*, 218B (2004) 17-33.

[11] P. Ulysse, Three-dimensional modeling of the friction stir-welding process, *International Journal of Machine Tools and Manufacture*, 42 (2002) 1549-1557.

[12] J. Goldak, A. Chakravarti and M. Bibby, A new finite element model for welding heat sources, *Metallurgical Transactions* (1983) 299-305.

[13] M. Khandkar, J. Khan and A. Reynolds, Input torque based thermal model of friction stir welding of Al-6061, *Trends in Welding Research, Proceedings of the 6th International Conference*, Callaway Gardens Resort, Phoenix, AZ, USA (2002) 218-223.

[14] F. Baratzadeh, Y. Tay, S. Patil and H. Lankarani, An experimental and numerical investigation into the dynamic crash testing of vehicle bumper fabricated using friction stir welding and gas metal arc welding, *International Journal of Crashworthiness* (2014) Doi: 10.1080/13588265.2014.904062.

[15] F. P. Incropera, D. P. DeWitt, T. L. Bergman and A. S. Lavine, *Fundamentals of heat and mass transfer*, John Wiley & Sons, Inc., 6 (2007).

[16] G. R. Johnson and W. H. Cook, A constitutive model and data for metal subjected to large strain, high strain rate and

high temperature, *Proceedings of 7th International Symposium on Ballistics*, The Hague, The Netherlands, April (1983) 541-548.
[17] G. R. Johnson and W. H. Cook, Fracture characteristics of three metals subjected to various strains, strain rates, temperatures and pressures, *Engineering Fracture Mechanics*, 21 (1) (1985) 31-48.
[18] J. O. Hallquist, *LS Dyna user's manual*, LSTC, version 971st, Troy, Michigan, 1 (2007).
[19] Z. H. Mir, K. J. A. Khandkar and A. P. Reynolds, Predicting residual thermal stresses in friction stir welded metals, *Journal of Materials Processing Technology*, 174 (2006) 195-203.
[20] L. Xu and J. A. Khan, Nugget growth model for aluminum alloys during resistance spot welding, *Welding Journal* (1999) 367-372.
[21] C. Madhusudana, *Thermal contact conductance*, Mechanical Engineering Series Book, Springer (1996).
[22] Livermore Software Technology Corporation, *Ls-Dyna keyword manual*, http://www.lstc.com.
[23] *ABAQUS analysis user's manual*, SIMULIA.
[24] R. V. Andrade, Pipe circularity reformation via line heating, *Thesis (S.M.)*, Massachusetts Institute of Technology, Dept. of Mechanical Engineering (2001).
[25] S. Patil, Y. Y. Tay, F. Baratzadeh and H. Lankarani, Modeling of friction-stir butt-welds and its application in automotive bumper impact performance Part 2. Impact modeling and bumper crash performance, *Journal of Mechanical Science and Technology*, 31 (7) (2017) 1-8.
[26] J. Y. Lim, M. J. Yoon, S. Y. Kim, H. S. Shin and T. G. Kim, Mechanical properties of CO2/MIG welded structural rolled steel and stainless steel, *Journal of Mechanical Science and Technology*, 29 (1) (2015) 103-108.

Sachin Patil is a doctoral student of Dr. Hamid Lankarani, Mechanical Engineering at Wichita State University. He has specialized in the application of explicit integration techniques for crashworthiness and impact weld failure problems. He has over 15 years of expertise in the field of Numerical Simulations, Sensitivity and Reliability Studies and have the distinction of being qualified as crash analyst with weld failure propagation. He has authored scholarly articles in the crashworthiness, optimization field, in professional as well as major trade publications and consult on the use of numerical simulations using LS-DYNA/ABAQUS.

Hamid Lankarani is a Professor of Mechanical Engineering and a Senior Fellow of the National Institute for Aviation Research at Wichita State University. He began his professional career in 1981. Dr. Lankarani is one of the world's leading researchers and educators in the field of impact dynamics, automotive and aircraft crashworthiness, occupant protection, and injury biomechanics.